



Contents lists available at ScienceDirect

Arabian Journal of Chemistry

journal homepage: www.sciencedirect.com



Original article

Revealing the effect of humic substance compounds on the aged characteristics and release compounds profiles from photodegradation of polyethylene microplastics

Minghong Xie^a, Deqing Ren^a, Atif Muhmood^b, Pengjiao Tian^a, Yingjie Su^c, Xiqing Wang^{a,*}^a College of Food Science Technology and Chemical Engineering, Hubei University of Arts and Science, Xiangyang, Hubei 441053, China^b Department of Agroecology, Aarhus University, Aarhus, Denmark^c Jilin Agricultural University, Changchun, Jilin Province, China

ARTICLE INFO

Article history:

Received 22 March 2023

Accepted 7 September 2023

Available online 12 September 2023

Keywords:

Humic acid

Fulvic acid

Microplastics

Degradation products

Photooxidation

ABSTRACT

The aim of this study was to investigate the effect of humic substance compounds (humic acid (HA) and fulvic acid (FA)) on the aged characteristics and release compounds profiles from polyethylene microplastics (PE-MPs). Results showed that HA promoted degree of PE-MPs photodegradation with a higher value of weight loss and oxygen atom and lower average particle size (110 μm), compared with the presence of FA during 15 days of irradiation. Likewise, the needle trap microextraction (HS-NTME) combined with gas chromatography/mass spectrometry (GC/MS) analysis revealed that HA and FA promoted a variety of oxygen-containing products (carboxyl acid, phenols and ketones) and siloxanes additives released from photodegradation of PE-MPs. Moreover, HA was found to have a higher ability to generate free radicals (·OH and O₂^{·-}) than FA, which accelerated the photooxidation of PE-MPs and led to the different mechanisms of photodegradation pathway of PE-MPs. These findings not only shed light on how humic substances affect photodegradation process of MPs, but also support further investigation into the possible hazard of MPs when co-existing compounds exist in the aqueous system.

© 2023 The Author(s). Published by Elsevier B.V. on behalf of King Saud University. This is an open access article under the CC BY-NC-ND license (<http://creativecommons.org/licenses/by-nc-nd/4.0/>).

1. Introduction

Due to their low cost and high durability, plastics are widely used in various industries, resulting in the generation of large amounts of plastic waste (Qiu et al., 2022; Tian et al., 2022). According to the United Nations Environment Programme (UNEP), there are between 75 million and 199 million tons of plastic waste in the oceans, accounting for 85% of the total weight of marine waste. Likewise, UNEP predicted that by 2040, the amount of plastic waste entering aquatic ecosystems would almost tripled, reaching 23 ~ 37 million tons per year (United Nations Environment Programme, 2021). Large amounts of plastic waste in the aquatic system are decomposed into smaller plastic fragments (Microplas-

tics, MPs) through various in-situ environment processes (e.g., photodegradation, biodegradation, and photooxidation) and released various harmful compounds during this process, posing a significant threat to socioeconomic, ecosystem, and human health (Wu et al., 2022; Zhu et al., 2022; Ding et al., 2022). Thus, it is necessary to assess the environmental hazards and behaviors of plastics in the aquatic system.

Although previous studies focused on monitoring abundance, distribution, and type of plastic pollution in aquatic systems (Han et al., 2020; Mao et al., 2021; Niu et al., 2021), recent research indicated that the potential concern associated with the release of harmful compounds during the degradation of plastics into the microplastics (Lomonaco et al., 2020; Wu et al., 2022). The release of harmful compounds, including volatile organic compounds (e.g., lactones, esters, and ketones), persistent organic pollutants (e.g., biphenyls, trichloroethane, and hexachlorobenzene), additives (e.g., plasticizers and colourants), and residual monomers, can result in secondary organic pollution and involve the physico-chemical reaction in the environment, leading to enhancing the toxicity effects in environment ecosystem (Hartikainen et al., 2018; Lomonaco et al., 2020). For instance, some persistent organic pollutants can generate the secondary organic aerosols or airborne

* Corresponding author.

E-mail address: xiqingwang91@163.com (X. Wang).

Peer review under responsibility of King Saud University.



Production and hosting by Elsevier

particles through the photooxidation process, further threaten aquatic organisms (Lomonaco et al., 2020; Wu et al., 2022). Likewise, Menicagli et al. (2019) reported that the volatile organic compounds negatively impacted the neuro-, hepato-, and nephrotoxicity of biota (Menicagli et al., 2019). Generally, releasing harmful compounds from plastics was significantly related to environmental factors (e.g., ultraviolet radiation and oxygen content) and coexisting active compounds.

Humic substances (HSs), are heterogeneous organic compounds that are mainly composed of humic acids (HAs), fulvic acids (FAs), and humins (HUs), the major organic fraction in soil, peat, dystrophic lakes, and ocean water (Ding et al., 2022; Guo et al., 2019). Among them, the HAs and FAs, as the main active compounds of HSs, contain a variety of functional groups (e.g., ketones and oxygen-containing functional groups) (The structural model shown in the Figure S1), contributing to reducing the bioavailability and toxicity and improving the transformation of inorganic/organic pollutants in the environment system (Tian et al., 2022). For instance, Tao et al. (2019) in their study confirmed that the two major functional groups (aryl C-O and alkyl ester C = O) of HA act as the main electron shuttles, which contributes to the biodegradation of dibutyl phthalate in mollisol (Tao et al., 2019). Likewise, our previous studies confirmed that HA with a higher electron transfer ability mediated the abiotic redox process of Cr (VI) under aerobic/anaerobic conditions, transferring high-valent to low-valent chromium and reducing toxicity (Wang et al., 2022; Wang et al., 2021). In recent years, the interfacial interaction between MPs and HAs/FAs has attracted attention, and the effect of HAs/FAs on the transport and retention behavior of MPs has generally been studied (Luo et al., 2022; Xi et al., 2022; Bogdanov et al., 2022). Ding et al. (2022) revealed from a molecular structure perspective that the oxygen-containing functional group in dissolved organic matters (HAs and FAs) is the main functional group affecting the transformation of MPs in environmental systems (Ding et al., 2022). Moreover, recent research has reported that HAs and FAs, as the reactive oxygen species generator, are involved in the photoaging of MPs in the aquatic system, accelerating the aging process (Qiu et al., 2022). Nonetheless, to date, information on the effect of HAs and FAs on the photodegradation behavior of MPs in aquatic systems, particularly the harmful compounds release from the photodegradation of MPs, is insufficient.

To fill this knowledge gap, this study has primarily investigated the effect of humic substances (HAs and FAs) on the degradation of microplastics under visible light conditions. Polyethylene microplastics (PE-MPs) were chosen as model plastics because of their broad applicability. The study aimed to (i) explore the effect of HAs and FAs on the degradation properties of PE-MPs under visible light conditions, (ii) clarify the release of degrading compounds from photoaging of PE-MPs under HAs and FAs addition conditions via needle trap microextraction (HS-NTME) combined with gas chromatography/mass spectrometry (GC/MS) analysis, and (iii) assess the potential environmental hazards of the degradation process of PE-MPs under the presence of HSs fractions.

2. Materials and methods

2.1. Chemical and materials

Polyethylene plastic was purchased from Liming Plastics Co., Ltd. (China), crushed using a grinder, and passed through a 100-mesh sieve. Humic acid (BR; CAS 1415-93-6) and fulvic acid (BR; CAS 479-66-3) was purchased from Shanghai Yuanye Bio-Technology Co., Ltd. (China). Other chemical reagents were purchased from Sigma-Aldrich Co. Ltd.

2.2. Batch experiment setup

In this study, laboratory-accelerated batch aging experiments were conducted in 40 ml quartz tubes with silica gel under a UV box (Fig. S2). The UV box is made of an opaque steel plate with two UV lamps (365 nm, Xujiang Electromechanical Inc., China) installed on the top. The light intensity in the exposure chamber was approximately 60 mW/cm², which was detected using a UV irradiation meter (Shenzhen Zhuoyue Yi Biao Co., Ltd., China). Likewise, the sample loaded vials were placed horizontally in the UV box. Before the aging experiments, the quartz tubes were treated in a muffle furnace at 500 °C for 4 h. Moreover, humic substances and MPs are substances present in large quantities in aqueous systems. Thus, as a representative of the natural environment, a 1:1 (w:w) ratio of MPs to HA and FA was chosen in this study and they were placed into the quartz tubes, respectively. Similarly, 30 ml of ultrapure water was added to the quartz tubes to simulate the environment within the aquatic system. The temperature of the chamber was maintained at 25 ± 3 °C. To investigate the evolution of the structure of PE-MPs and the release of degradation compounds, tube samples were taken at time points of 0, 3, 6, 9, 12, and 15 days. The control treatment groups were subjected to the same conditions without HA and FA addition. The treatment and control groups were taken in triplicate.

2.3. Characterization of the microplastics

MPs were extracted from samples collected at each time point for characterization. Briefly, the samples were shaken at 150 rpm for 24 h with 5 M NaCl solution at a 1:3 (v:v) ratio. The supernatant was separated from the mixed solution by centrifugation at 5000 rpm for 10 min. Finally, the supernatants were subjected to solid-liquid separation through a glass microfiber filter, and then the solid phase was treated by the dehybridization process. The solid phase was first rinsed three times with methanol and filtered to remove degradation products that might have adhered to the surface. The solid phase fraction was then mixed with 30% hydrogen peroxide solution for 12 h and filtered to remove the HA and FA absorbed on the surface of the MPs. Finally, the collected MPs were oven-dried (50 °C, 2 h) for surface morphology and chemical bonding characterization. In this study, the surface morphology variability of pristine and degraded MPs was analyzed using a scanning electron microscopy-energy dispersive spectrometer (SEM-EDS, SU8020, Japan). The evolution of the PE-MP particle size was further analyzed using a laser particle size analyzer (LPSA). Similarly, X-ray photoelectron spectroscopy (XPS, Thermoescalab 250Xi, USA) was used to determine and analyze the changes in the chemical bonding of PE-MPs throughout the degradation process. High-resolution C 1 s and O 1 s regions were recorded in the XPS spectra.

2.4. Determination of the free radicals

The free radicals (●OH) of the samples were determined using electron paramagnetic resonance spectroscopy (EPR, A300-10/12, Bruker, Germany) according to the method recommended by Xing et al. (2022). Briefly, approximately 9 ml samples collected at different irradiation times were mixed with 1 ml of 5,5-dimethyl-1-pyrroline-N-oxide (0.03 M) in the dark and stirred for 2 min. The mixed system was then filtered through a 0.45 μm filter membrane and analyzed by EPR spectrometry at room temperature. The operating parameters of the EPR instrument were as follows: microwave power, 10mW; modulation amplitude 2.071 G; sweep width, 100G; center field, 3480 G; sweep time, 41.943 s. Furthermore, to analyze the content of ●OH in the photodegradation process of PS-MPs, high-performance liquid chromatography

(HPLC, Agilent 1200) was used in this study (Qiu et al., 2022). The samples (5 ml) collected at different irradiation times were mixed with sodium benzoic acid (0.01 M) in the dark and stirred for 20 min. Then, a 2 ml mixture was filtered, and the ■OH content was determined by monitoring the p-hydroxybenzoic acid content using HPLC.

2.5. Analysis of the release of the degradation compounds

The degradation compounds from the MP aging process were determined by headspace-solid phase microextraction coupled with gas chromatography-mass spectrometry (GC/MS). In this study, the liquid fraction of the sample and methanol wash phase (degradation products attached to the MPs surface) were combined for analysis of degradation compounds. The degradation compounds were extracted according to the standard method described by Wu et al. (2022). Briefly, the liquid phase was first obtained using the headspace-solid phase microextraction. A 10 ml sample was transferred to a 20 ml headspace vial and subjected to solid phase microextraction at 80°C. The adsorption time was 40 min, and the test was performed after desorption at 250 °C for 3 min. GC-MS analysis was carried out using GC-MS QP2010 ultra (Shimadzu, Kyoto, Japan) with the DB-5MS Column (Agilent, J&W Scientific, 30 m \times 0.25 mm \times 0.25 μm). Helium was used as carrier gas with a constant flow rate of 1 ml/min. The temperature program started at 40 °C for 2 min, rose to 200 °C with a rate of 6 °C/min, and then to 300 °C with a rate of 15 °C (3 min hold time). The temperature of the inlet, transfer line, and ion source was set to 250 °C, 280 °C, and 220 °C, respectively. MS acquisition was performed with the range of 33–500 mass units. The extracted peaks

were identified by NIST 14 library and ones with matching degrees higher than 800 were marked.

3. Results and discussion

3.1. Characteristics of the surface properties

Previous studies have confirmed that MPs undergo significant changes in their physical properties, including surface characteristics, weight loss, and particle size, during the aging/degradation process (Zhang et al., 2022; Zhu et al., 2022). Thus, to investigate the effect of HA and FA on the photodegradation of PE-MPs, the surface characteristics of PE-MPs were first determined using a scanning electron microscopy-energy dispersive spectrometer (SEM-EDS). A significant difference in the surface morphology between the initial and aged PE-MPs was observed in this study (Fig. 1). The results showed that the surface morphology of the initial PE-MPs was relatively smooth and shiny (Fig. 1a). However, the surface properties of PE-MPs without interaction with HA and FA became relatively rough after 15 d of irradiation (Fig. 1c). Moreover, when HA and FA were involved, some cracks and holes were observed in the surface properties of the PE-MPs (Fig. 1 b and d). The significant changes in the surface properties of the PE-MPs may be due to the shrinkage and reorganization of the structure due to the removal of photodegradation by-products, thus leading to cracks (Nanoparticle and Nabi, 2020; Uheida et al., 2021). Likewise, the presence of cracks increases the degree of degradation because it provides a pathway for oxygen to penetrate deeper into the PE-MPs and enhance photo-oxidation, resulting in the appearance of holes on the surface of the PE-MPs (Yang et al., 2022).

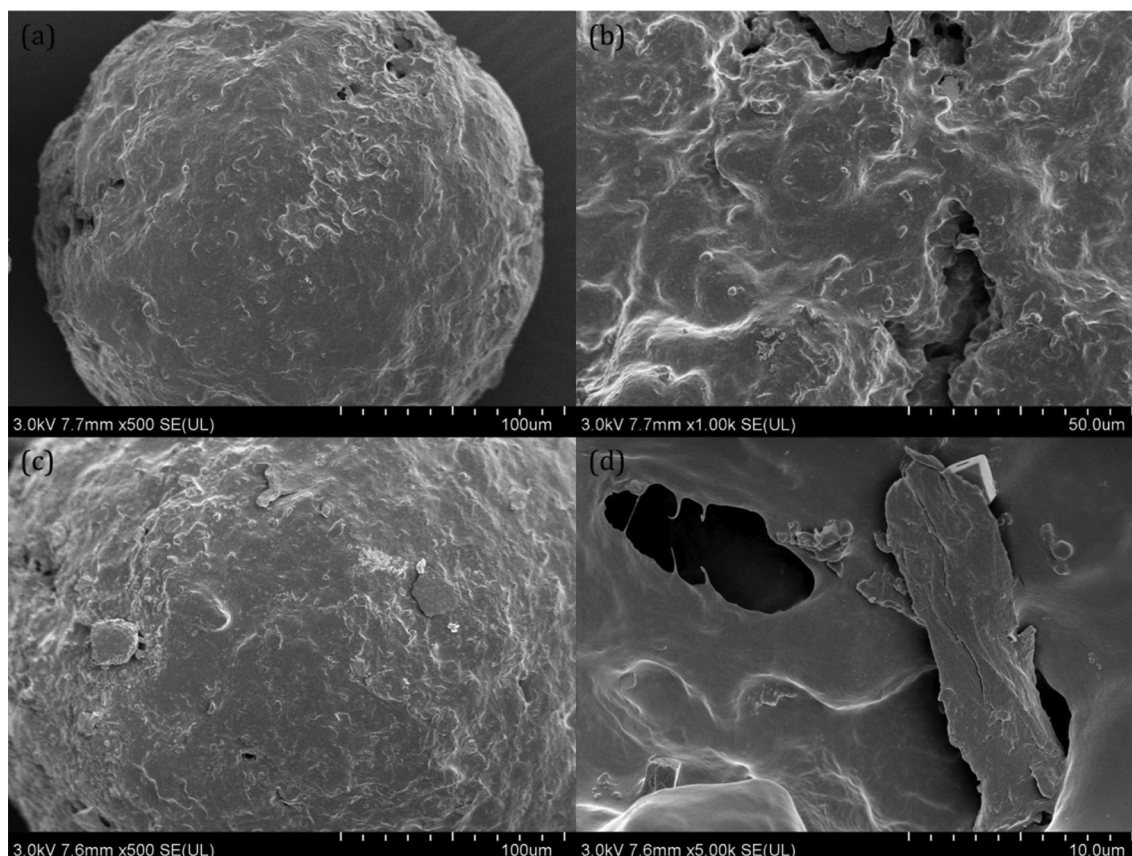


Fig. 1. The change in the physical properties of the PE-MPs after 15 d of irradiation. (a) the SEM image of the initial PE-MPs; (b) the SEM image of the aged PE-MPs with fulvic acid; (c) the SEM image of the aged PE-MPs without humic acid and fulvic acid; (d) the SEM image of the aged PE-MPs with humic acid.

3.2. Characteristics of the physical properties

Moreover, the physical properties, including weight loss and particle size of the PE-MPs are also commonly used to characterize the degradation efficiency under irradiation conditions, although the degradation of PS-MPs is slower under natural conditions (Chen et al., 2021; Yang et al., 2015). The weight loss of PS-MPs in the absence and presence of HA and FA was determined (Fig. 2a). Results showed that the average weight loss of aged PE-MPs without HA and FA was 1.28%, which was 159% and 288%

lower than weight loss during the degradation process with FA (3.31%) and HA (4.96%). Previous studies have demonstrated that the weight loss of PE-MPs is only in the range of 0.005% to 1.5% under UV condition (Chen et al., 2021). This may be due to the photodegradation and photooxidation of the PE-MPs under UV conditions. Moreover, compared with the presence of FA, a higher weight loss of aged PE-MPs was observed in the presence of HA when irradiated for 15 days, indicating that HA might promote the degree of photodegradation and photooxidation process of PE-MPs.

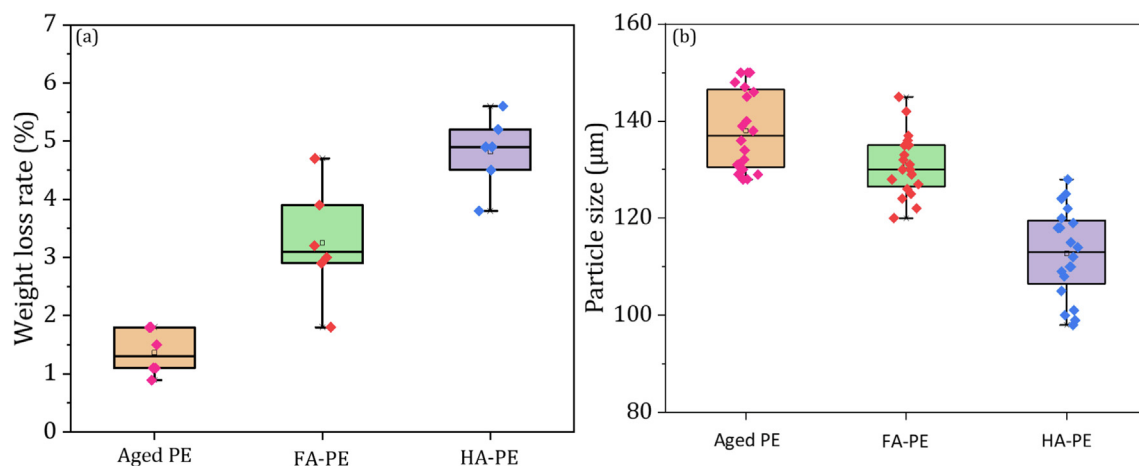


Fig. 2. The dry weight loss (a) and average size distributions (b) of the PE-MPs after 15 d of irradiation.

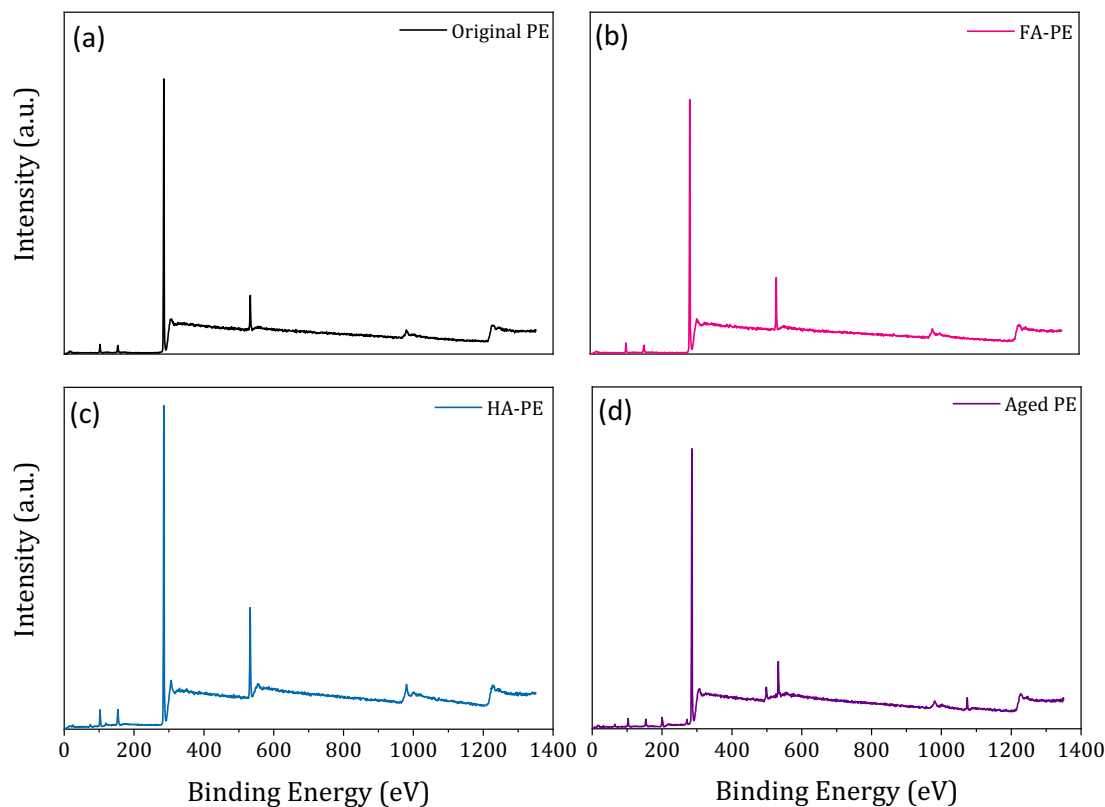


Fig. 3. The X-ray photoelectron spectroscopy spectra of original PE (a), aged PE-MPs with the presence of FA (b), aged PE-MPs with the presence of HA (c), and aged PE-MPs without FA and HA (d).

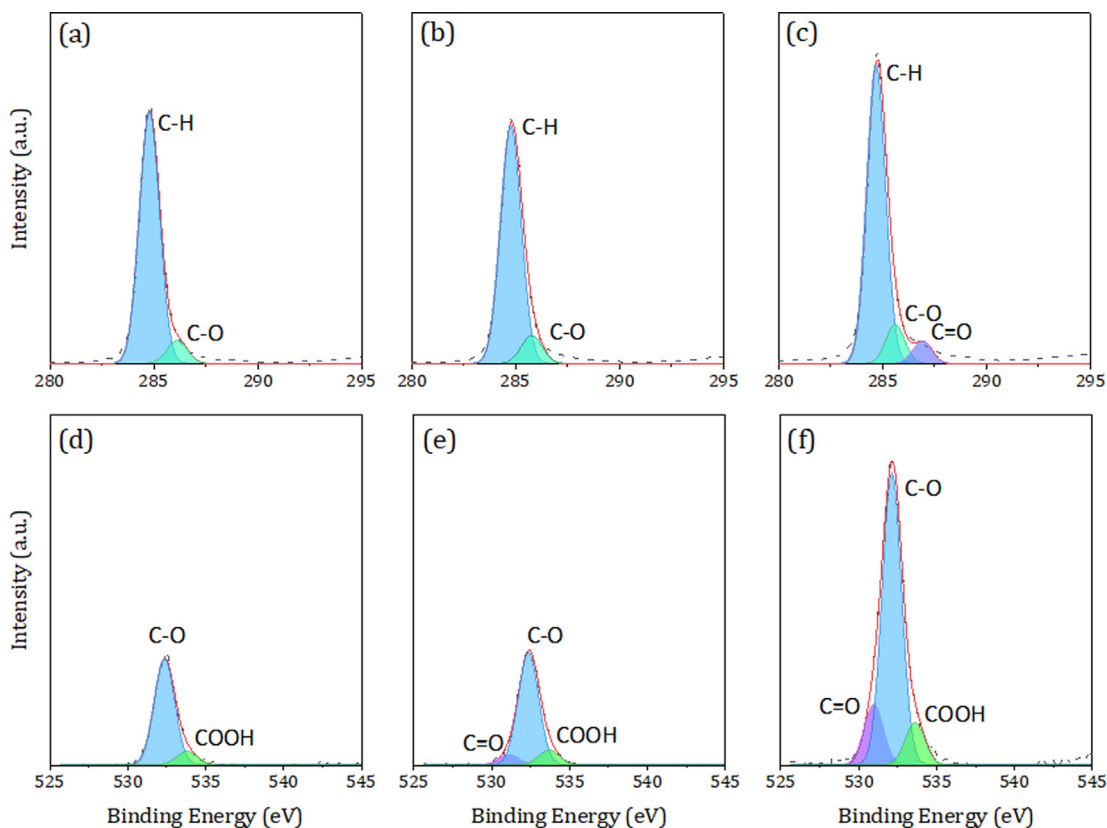


Fig. 4. The X-ray photoelectron spectroscopy C 1 s and O 1 s spectra of aged PE-MPs without FA and HA (a and d), aged PE-MPs with the presence of FA (b and e), aged PE-MPs with the presence of HA (c and f).

Furthermore, the evolution of the PE-MP particle size was determined using a laser particle size analyzer (Fig. 2b). A decreasing trend in the particle size distribution of PE-MPs was observed during photodegradation. The average particle size of the aged PE-MPs was 148 μm . After irradiation for 15 days, the average particle size of aged PE-MPs without HA and FA participation decreased from 148 μm to 136 μm (approximately 8.1%). In the presence of FA, the average particle size of the PS-MPs decreased to 129 μm , which was 12.8% and 5.2% lower than that in the original and without the addition of FA, respectively. Compared with the presence of FA, a lower average particle size of aged PE-MPs was observed in the presence of HA (110 μm). This might be attributed to the enhanced chain break and degradation of PE-MPs during irradiation for 15 days. The decrease in the particle size of the PE-MPs during photodegradation might be the reason for the increased weight loss. Moreover, the PE-MPs showed a smaller particle size distribution in the photodegradation process with HA and FA participation than that without HA and FA participation. These results indicate that HA and FA may promote the photodegradation of PE-MPs, especially the presence of HA may contribute to the breakage and degradation of chain and surface structure.

3.3. Evolution of the chemical properties

The photodegradation of MPs is usually accompanied by photooxidation, resulting in a change in the chemical bonds. Thus, to evaluate the influence of HA on the photodegradation of the PE-MPs, XPS analysis was used to characterize the evolution of the chemical bonds (Fig. 3). In the original PS-MPs, a small content of oxygen atoms was observed, suggesting that a low degree of oxida-

tion had occurred on the surface of the PE-MPs during the production, crushing, and storage processes (Chen et al., 2020, 2021). When compared to the original PE-MPs, higher levels of oxygen atoms were observed in the aged PE-MPs, indicating a higher degree of oxidation under light irradiation conditions (Xing et al., 2022). Moreover, the XPS spectra of aged PE-MPs exhibited significant differences in the presence of HA and FA. The O 1 s peak value of the photodegradation of PE-MPs with HA was higher than that in the presence of FA.

Furthermore, the XPS C 1 s and O 1 s spectra of PE-MPs were conducted by peak fitting (Fig. 4). A significant difference was observed in aged PE-MPs without and with the presence of FA and HA. In the C 1 s of the spectrum of aged PE-MPs without the presence of FA and HA, two peaks at 284.9 eV and 286.5 eV, corresponding to the C-H and C-O groups were observed, indicating that long-chain structure breakage and oxidation occurred during the photodegradation process (Chen et al., 2020). There was no significant difference in aged PE-MPs with the presence of FA. However, in the C 1 s of the spectrum of aged PE-MPs with the presence of HA, additional C = O peaks (287.3 eV) appeared. Likewise, the area of C-H and C-O of aged PE-MPs with the presence of HA was higher than aged PE-MPs with and without the presence of FA. In the peak fitting of the high-resolution XPS spectra of the O 1 s regions, it can be concluded that the two peaks at 533.1 eV and 534.2 eV of the aged PE-MPs without the presence of FA and HA, corresponding to the C-O and COOH groups, indicating that the surface chemical bonds of the PS-MPs were oxidized to carboxylic type compounds (Al Abdual et al., 2015). While additional C = O (531.5 eV) appeared in the aged PE-MPs with the presence of FA and HA compared to the aged PE-MPs without the presence of FA and HA. Further analysis of the effect of HA and FA on the photodegradation

process of PE-MPs revealed a higher content of oxygen-containing functional groups (COOH, C-O, C = O) in the aged PS-MPs with the presence of HA than in the presence of FA, indicating that HA can contribute to the higher degree of photooxidation of the PE-MPs. Furthermore, the carbonyl index (CI) and O/C ratio are important indicators that have been widely used to quantitatively characterize the degree of oxidation of MPs (Yang et al., 2022; Liu et al., 2019). Generally, the CI value and O/C ratio are significantly positively correlated with the oxidation degree of MPs (Rouillon et al., 2016). In this study, the CI value of the PE-MPs in the presence of HA after irradiation for 15 days (0.75) was higher than that of the aged PE-MPs (0.08) without the presence of HA and FA, and aged PE-MPs in the presence of FA (0.41). These findings are consistent with the results from previous studies. Likewise, we also found that the CI value of PS-MPs in the presence of HA after irradiation for 40 days was 0.53 in our already conducted study (Wang et al., 2023). Similarly, the O/C ratio showed a trend similar to that of the CI value (Table 1). These results suggest that HA, as an excellent free radical generator and electron transfer carrier, may easily mediate the photooxidation of PE-MPs in the photodegradation process (Qiu et al., 2022).

Table 1
The carbonyl index and O/C ratio of aged PE-MPs during the photodegradation process.

Parameters	Original PE-MPs	Aged PE-MPs without HA and FA	Aged PE-MPs with HA	Aged PE-MPs with FA
Carbonyl index	0.019	0.08	0.75	0.41
O/C ratio	0.015	0.03	0.07	0.05

3.4. Characteristics of the degradation products

To further verify the potential hazards of aged PE-MPs under the presence of HA and FA, the degradation products were determined via the headspace with needle trap microextraction (HS-NTME) combined with gas chromatography/mass spectrometry (GC/MS). It was perceived that the differences in HS-NTME-GC/MS spectra were observed after a retention time from 10 to 30 min (Fig. 5 a-c and Fig. S4). In the chromatogram of aged PE-MPs without the presence of HA and FA, a large number of siloxanes (e.g., cyclopentasiloxanes, cyclohexasiloxanes, cycloheptasiloxanes, cyclooctasiloxanes, and cyclononasiloxanes) and a small number of aldehyde and amide degradation products (e.g., nonanal, benzaldehyde, 2,4-di-*tert*-butylphenol, and octadecanamide) were observed. Among them, siloxane products being important raw materials and additives in the plastics production process, were released to the environment in large amounts during the chain breaks of photodegradation of PE-MPs (Rani et al., 2017; Suhrhoff and Scholz-Bottcher, 2016). Meanwhile, the presence of small amounts of aldehyde and amide degradation products suggests that photo-oxidation processes occur during the photodegradation of PE-MPs (Wu et al., 2022; Dong et al., 2019). In the chromatogram of aged PE-MPs with the presence of FA, additional peaks at 19.924, 20.382, 22.524, and 28.613 min/RT, corresponding to the 2-propenoic acid, phenol, heptadecane, methanone /phenyl (3-tridecyloxiranyl) were observed. Moreover, the relative content of siloxane products was higher in aged PE-MPs with HA and FA than that of without the presence of HA and FA. This result suggests that the presence of FA may promote the photodegradation process of PE-MPs. However, the extent of its influence on the photooxidation process of PE-MPs could not be determined from the product perspective of this study. Compared with the presence of FA, additional peaks at 10.559, 11.535, 15.970, 17.236, 19.167,

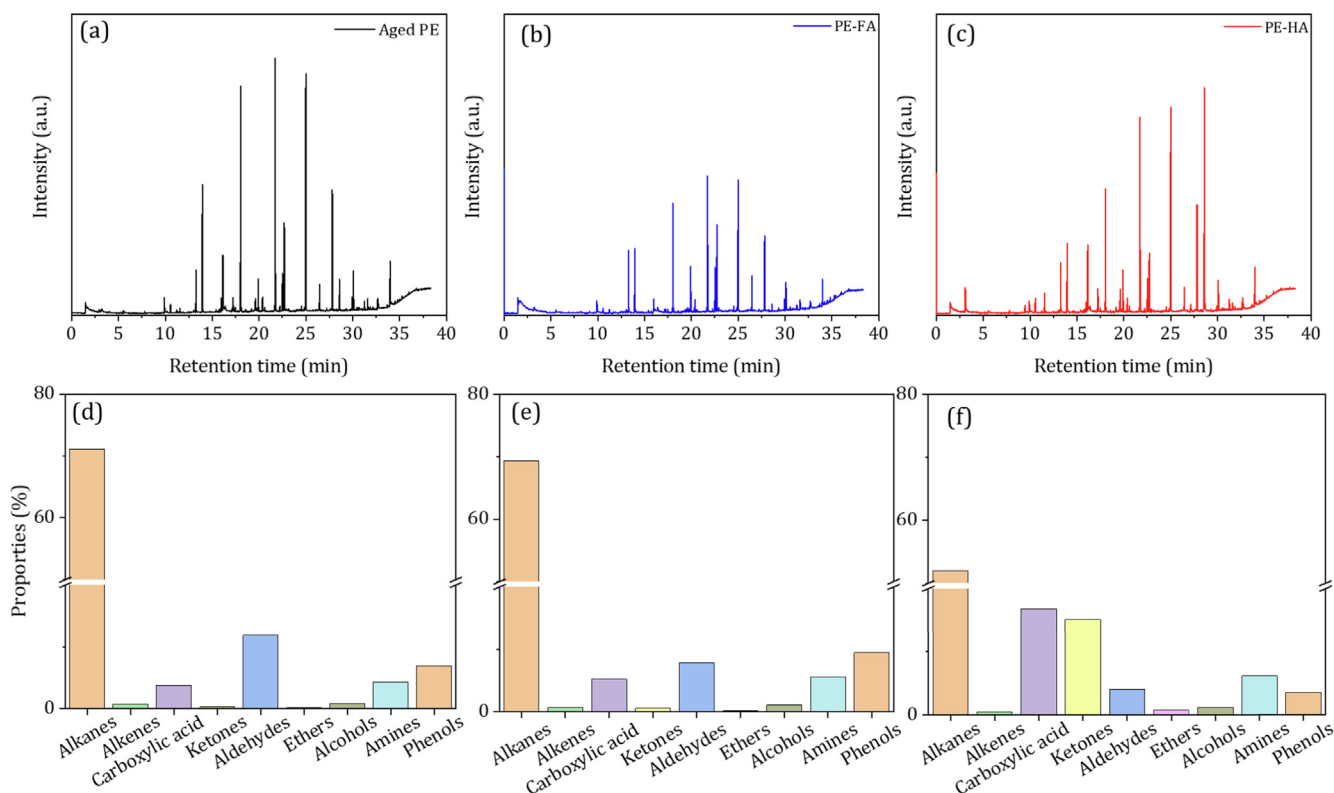


Fig. 5. The HS-NTME-GC/MS total ion chromatograms and overview of the chemical group pattern of products of aged PE-MPs with the presence of HA and FA (a and d), aged PE-MPs with the presence of FA (b and e), aged PE-MPs with the presence of HA (c and f).

19.610, 24.543, 27.146, 28.602 min/RT, corresponding to octanal, benzenemethanamine, ether, 2-decenal, 2,2,6,7-tetramethyl-10-oxatricyclo, 2-undecenal, nonadecane, ethanone, propanetrione were found in the aged PE-MPs with the presence of HA. Also, more aldehydes, ketones, amines and alkanes were found, suggesting that the presence of HA may promote a higher degree of chain breaking and photo-oxidation of PE-MPs.

Furthermore, based on the total HS-NEME-GC/MS ion chromatograms and the structure of those degradation products, nine product types were identified in this study, including alkanes, alkenes, carboxylic acid, ketones, aldehydes, ethers, alcohols, amines, and phenols (Fig. 5 d-f). Results showed a significant difference in the relative content of products in the different groups. In the aged PE-MPs without the presence of HA and FA, the relative content of alkanes, alkenes, carboxylic acid, ketones, aldehydes, ethers, alcohols, amines, and phenols were 71.1%, 0.7%, 3.8%, 0.2%, 11.9%, 0.1%, 0.8%, 4.3%, and 6.9%, respectively. While, in the aged PE-MPs with the presence of FA, the relative content of alkanes, alkenes, carboxylic acid, ketones, aldehydes, ethers, alcohols, amines, and phenols were 69.4%, 0.7%, 5.2%, 0.5%, 7.8%, 0.1%, 0.1%, 5.6%, and 9.4%, respectively. These findings indicated that FA may con-

tribute the oxygen-containing product generation, such as carboxylic acid and phenols. Compared to the aged PE-MPs with the presence of FA, higher content of the oxygen-containing products including carboxylic acid (16.8%) and ketones (15.1%) were observed in the aged PE-MPs with the presence of HA process. This result demonstrated that HA has a higher oxidative capacity than FA to promote the photooxidative degradation of PE-MPs, which might be due to its higher free radical generation capacity (Liu et al., 2019; Wu et al., 2021).

3.5. Potential mechanism of PE-MPs photodegradation under humic substances

Previous studies reported that the photodegradation degree of MPs was significantly related to the reactive oxygen species (ROS) in the reaction system (Wu et al., 2021). Generally, the chemical bonds (e.g., C-C and C-H) in MPs are broken under the stimulation of light irradiation, resulting in the generation of ROS from MPs (Qiu et al., 2022), which further contributed to the breakage and oxidation of MPs. Recently it was observed that ROS can also be formed from polymers with conjugated benzene ring struc-

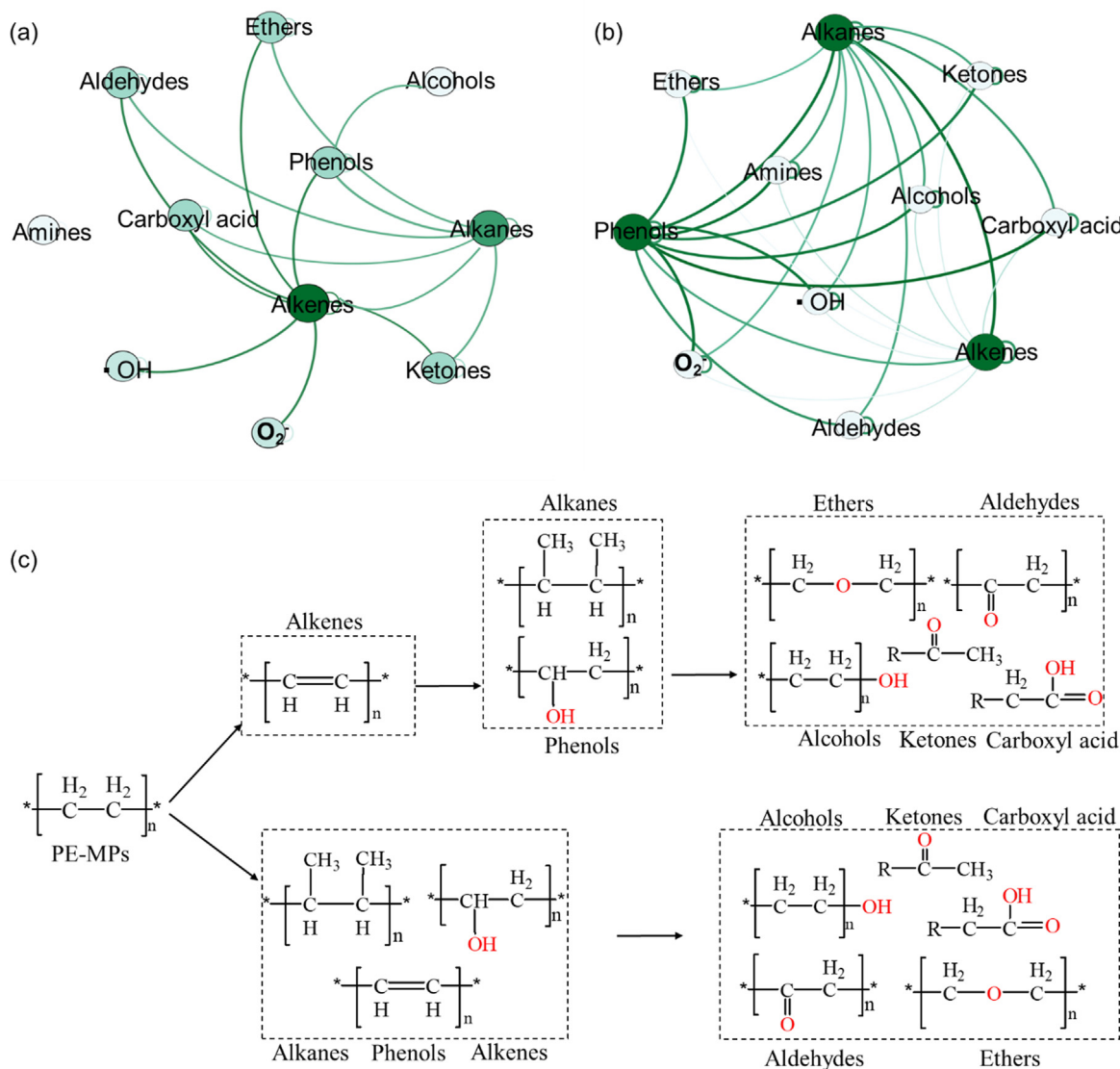


Fig. 6. Co-occurrence network of the reactive oxygen species (●OH and O₂) indices indicating the degradation products during the presence of FA (a) and HA (b). The differential intensities of the green connections in the visualized co-occurrence network represent significant correlations between the measured parameters. (c) Possible influence of HA and FA on the photodegradation pathway of PE-MPs.

tures (e.g., humic substances and lignin). Thus, to explore the potential mechanisms of photodegradation of PE-MPs under the involvement of HA and FA, the ROS was determined via the EPR analysis combined with DMPO as the spin-trapping agent (Fig. S3). Results showed that the characteristic peaks signals of EPFRs including DMPO- \bullet OH and DMPO- O_2^- were detected on the surface of the aged PE-MPs isolated from the aging process in the presence of FA and HA, whereas negligible signals of DMPO- \bullet OH and DMPO- O_2^- were determined on the pristine PE-MPs surface. This finding indicated that \bullet OH and O_2^- were produced in the aging system under the FA and HA. EPFRs could also form on MPs under conditions of high temperature and light irradiation as previously reported, thereby inducing the generation of ROS, including \bullet OH and O_2^- through the transfer of electrons to H_2O or O_2 , and these ROS could further accelerate the aging of MPs (Zhu et al., 2020a, 2020b; Ding et al., 2020). In addition, an increasing trend in \bullet OH and O_2^- generation was observed in the photodegradation process of PE-MPs in the presence of FA and HA. In the presence of FA, the average \bullet OH and O_2^- values reached 0.204 mM and 0.185 mM after irradiation for 15 days, respectively. When compared to photodegradation in the presence of FA, a significantly higher \bullet OH and O_2^- yield (0.431 mM and 0.293 mM respectively) was observed during the photodegradation of PS-MPs with the HA after 15 days of irradiation. According to previous studies, the generation of \bullet OH and O_2^- from HA is divided into two main pathways. First, a small amount of ROS is generated spontaneously, mainly from the stabilized reactive radical functional groups on the surface of the HA structure. Moreover, HA, as an electron shuttle carrier, mediates electron transfer during redox reactions within the system, thereby promoting the generation of ROS. Thus, the higher ROS contents found in the presence of HA under UV conditions may be due to the photoelectron stimulation accelerated the reaction rate of HA spontaneous and electron transfer. These results confirmed that the production of ROS by HA/FA-mediated redox transformation on the surface of PE-MPs is the main driving force for MPs aging under UV conditions. Thus, a stronger intensity of ROS formation from the PE-MPs with the HA system may lead to significant differences in the degradation pathway of PS-MPs without HA.

Furthermore, in order to verify this hypothesis, the relationship between ROS and degradation products was analyzed by the co-occurrence network analysis (Fig. 6). As shown in Fig. 6 a and b, in the visualized co-occurrence networks, the difference intensity of green connection represents significant correlations between the measured parameters. In detail, the ROS (\bullet OH and O_2^-) formed from FA was significantly positively correlated with the alkenes, while the ROS (\bullet OH and O_2^-) formed from HA was significantly positively correlated with the phenols and alkanes. This result suggests that the presence of ROS from FA may contribute to chain breakage as well as a low degree of oxidative dehydrogenation reactions in the first place, while the production of higher value ROS from HA contributes more to the breakage of PE-MPs as well as to the oxidative process. Furthermore, in the degradation of PE-MPs involving HA, the results showed that the amount of phenolic production have a significant positive correlation with oxygenated products, such as alcohols, esters, ketones, aldehydes and carboxylic acids. However, in the degradation of PE-MPs involving FA, olefins were the precursors of oxygenated products. This result suggests that HA and FA may mediate different photodegradation processes of PE-MPs (Fig. 6 c).

4. Conclusions

MPs and humic substances are ubiquitous in aquatic systems. To better understand the effects of humic substances on the pho-

todegradation of MPs humic acid (HA) and Fulvic acid (FA) were selected as representative examples to investigate the aged characteristics and release compounds profiles during the photodegradation of PE-MPs. The results showed that HA and FA promoted weight loss and the generation of the aged PS-MPs with smaller particle sizes during 15 days of irradiation. Likewise, this study revealed that HA and FA promoted a variety of oxygen-containing products (carboxyl acid, phenols and ketones) and siloxanes additives released from the photodegradation of PE-MPs. Moreover, HA was found to have a higher ability to generate free radicals (\bullet OH and O_2^-) than FA, which accelerated the photooxidation of PE-MPs and led to the different mechanisms of the photodegradation pathway of PE-MPs. The findings of the current study can serve as a baseline in evaluating how coexisting pollutants affect photodegradation of MPs in the aquatic system.

Declaration of Competing Interest

The authors declare that they have no known competing financial interests or personal relationships that could have appeared to influence the work reported in this paper.

Acknowledgments

This work was supported by the Natural Science Foundation of Hubei Province Cultivation Program, China (2022CFD096), Xiangyang City Science and Technology Bureau Project, Hubei Province, China (2022ABA006208), Hubei University of Arts and Science, Hubei Province, China (S202210519009) and Ministry of Education of the People's Republic of China Research, China (202201618).

Appendix A. Supplementary material

Supplementary data to this article can be found online at <https://doi.org/10.1016/j.arabjc.2023.105257>.

References

- Bogdanov, K.I., Kostina, N.V., Plakunov, V.K., Zhurina, M.V., 2022. Effect of humic acid on biofilm formation on polyethylene surface and its biodegradation by soil bacteria. *Soil Biol.* 55, 474–484.
- Chen, G., Feng, Q., Wang, J., 2020. Mini-review of microplastics in the atmosphere and their risks to humans. *Sci. Total Environ.* 703. <https://doi.org/10.1016/j.scitotenv.2019.135504> 135504.
- Chen, S., Yang, Y., Jing, X., Zhang, L., Chen, J., Rensing, C., Luan, T., Zhou, S., 2021. Enhanced aging of polystyrene microplastics in sediments under alternating anoxic-oxic conditions. *Water Res.* 207. <https://doi.org/10.1016/j.watres.2021.117782> 117782.
- Ding, L., Mao, R., Ma, S., Guo, X., Zhu, L., 2020. High temperature depended on the aging mechanisms of microplastics under different environmental conditions and its effect on the distribution of organic pollutants. *Water Res.* 174, 115634.
- Ding, L., Luo, Y., Yu, X., Ouyang, Z., Liu, P., Guo, X., 2022. Insight into interactions of polystyrene microplastics with different types and compositions of dissolved organic matter. *Sci. Total Environ.* 824. <https://doi.org/10.1016/j.scitotenv.2022.153883> 153883.
- Dong, H., Jiang, L., Shen, J., Zhao, Z., Wang, Q., Shen, X., 2019. Identification and analysis of odor-active substances from PVC-overlaid MDF. *Environ. Sci. Pollut. Res.* 26, 20769–20779. <https://doi.org/10.1007/s11356-019-05263-2>.
- Guo, X., Liu, H., Wu, S., 2019. Humic substances developed during organic waste composting: Formation mechanisms, structural properties, and agronomic functions. *Sci. Total Environ.* 662, 501–510. <https://doi.org/10.1016/j.scitotenv.2019.01.137>.
- Han, M., Niu, X., Tang, M., Zhang, B., Wang, G., Yue, W., 2020. Distribution of microplastics in surface water of the lower Yellow River near estuary. *Sci. Total Environ.* 707. <https://doi.org/10.1016/j.scitotenv.2019.135601> 135601.
- Hartikainen, A., Yli-pirila, P., Tiitta, P., Leskinen, A., Kortelainen, M., Orasche, J., Schnelle-kreis, J., Lehtinen, K.E.J., Zimmermann, R., Jokiniemi, J., 2018. Volatile organic compounds from logwood combustion: Emissions and transformation under dark and photochemical aging conditions in a Smog Chamber. *Environ. Sci. Tech.* 52 (8), 4979–4998. <https://doi.org/10.1021/acs.est.7b06269>.
- Liu, P., Qian, L., Wang, H., Zhan, X., Lu, K., Gu, C., Gao, S., 2019. New insights into the aging behavior of microplastics accelerated by advanced oxidation process. *Environ. Sci. Tech.* 53, 3579–3588.

- Lomonaco, T., Manco, E., Corti, A., Nasa, J.L., Ghimenti, S., Biagini, D., Francesco, F.D., Modugno, F., Ceccarini, A., Fuoco, R., 2020. Release of harmful volatile organic compounds (VOCs) from photo-degraded plastic debris: A neglected source of environmental pollution. *J. Hazard. Mater.* 394,. <https://doi.org/10.1016/j.jhazmat.2020.122596> 122596.
- Luo, H., Liu, C., He, D., Sun, J., Zhang, A., Li, J., Pan, X., 2022. Interactions between polypropylene microplastics (PP-MPs) and humic acid influenced by aging of MPs. *Water Res.* 222, 118921.
- Mao, R., Song, J., Yan, P., Ouyang, Z., Wu, R., Liu, S., Guo, X., 2021. Horizontal and vertical distribution of microplastics in the Wuliangshuai Lake sediment, northern China. *Sci. Total Environ.* 754,. <https://doi.org/10.1016/j.scitotenv.2020.142426> 142426.
- Menicagli, V., Balestri, E., Lardicci, C., 2019. Exposure of coastal dune vegetation to plastic bag leachates: A neglected impact of plastic litter. *Sci. Total Environ.* 683, 737–748. <https://doi.org/10.1016/j.scitotenv.2019.05.245>.
- Nanoparticle, T., Nabi, I., 2020. iScience II Complete Photocatalytic Mineralization of. *ISCIENCE* 23, 101326. <https://doi.org/10.1016/j.isci.2020.101326>.
- Niu, L., Li, Y., Li, Y.I., Hu, Q., Wang, C., Hu, J., Zhang, W., Wang, L., Zhang, C., Zhang, H., 2021. New insights into the vertical distribution and microbial degradation of microplastics in urban river sediments. *Water Res.* 188,. <https://doi.org/10.1016/j.watres.2020.116449> 116449.
- Qiu, X., Zhang, J., Fang, L., Guo, X., Zhu, L., 2022. Dissolved organic matter promotes the aging process of polystyrene microplastics under dark and ultraviolet light conditions: The crucial role of reactive oxygen species. *Environ. Sci. Tech.* 56 (14), 10149–10160. <https://doi.org/10.1021/acs.est.2c03309>.
- Rani, M., Shim, W.J., Jang, M., Han, G.M., Hong, S.H., 2017. Releasing of hexabromocyclododecanes from expanded polystyrenes in seawater -field and laboratory experiments. *Chemosphere* 185, 798–805. <https://doi.org/10.1016/j.chemosphere.2017.07.042>.
- Suhrhoff, T.J., Scholz-Böttcher, B.M., 2016. Qualitative impact of salinity, UV radiation and turbulence on leaching of organic plastic additives from four common plastics—a lab experiment. *Mar. Pollut. Bull.* 102, 84–94. <https://doi.org/10.1016/j.marpolbul.2015.11.054>.
- Tao, Y., Shi, H., Jiao, Y., Han, S., Akindolie, M.S., Yang, Y., 2019. Effects of humic acid on the biodegradation of di-n-butyl phthalate in mollisol. *J. Clean. Prod.* 249,. <https://doi.org/10.1016/j.jclepro.2019.119404> 119404.
- Tian, P., Muhmood, A., Xie, M., Cui, X., Su, Y., Gong, B., Yu, H., Li, Y., Fan, W., Wang, X., 2022. New insights into the distribution and interaction mechanism of microplastics with humic acid in river sediments. *Chemosphere* 307,. <https://doi.org/10.1016/j.chemosphere.2022.135943> 135943.
- Uheida, A., Giraldo, H., Abdel-rehim, M., Hamd, W., Dutta, J., 2021. Visible light photocatalytic degradation of polypropylene microplastics in a continuous water flow system. *J. Hazard. Mater.* 406,. <https://doi.org/10.1016/j.jhazmat.2020.124299> 124299.
- United Nations Environment Programme (2021). *From Pollution to Solution: A global assessment of marine litter and plastic pollution*. Nairobi.
- Wang, X., Lyu, T., Dong, R., Liu, H., Wu, S., 2021. Dynamic evolution of humic acids during anaerobic digestion: Exploring an effective auxiliary agent for heavy metal remediation. *Bioresour. Technol.* 320,. <https://doi.org/10.1016/j.biortech.2020.124331> 124331.
- Wang, X.Q., Muhmood, A., Ren, D., Tian, P., Li, Y., Yu, H., Wu, S., 2023. Exploring the mechanisms of humic acid mediated degradation of polystyrene microplastics under ultraviolet light conditions. *Chemosphere* 327, 138544.
- Wang, X., Tian, P., Muhmood, A., Liu, J., Su, Y., Zhang, Q., Zheng, Y., Dong, R., 2022. Investigating the evolution of structural characteristics of humic acid generated during the continuous anaerobic digestion and its potential for chromium adsorption and reduction. *Fermentation* 8, 322.
- Wu, X., Liu, P., Gong, Z., Wang, H., Huang, H., Shi, Y., Zhao, X., Gao, S., 2021. Humic acid and fulvic acid hinder long-term weathering of microplastics in lake water. *Environ. Sci. Tech.* 55, 15810–15820.
- Wu, X., Chen, X., Jiang, R., You, J., Ouyang, G., 2022. New insights into the photo-degraded polystyrene microplastic: Effect on the release of volatile organic compounds. *J. Hazard. Mater.* 431,. <https://doi.org/10.1016/j.jhazmat.2022.128523> 128523.
- Xi, B., Wang, B., Chen, M., Lee, X., Zhang, X., Wang, S., Yu, Z., Wu, P., 2022. Environmental behaviors and degradation methods of microplastics in different environmental media. *Chemosphere* 299,. <https://doi.org/10.1016/j.chemosphere.2022.134354> 134354.
- Xing, R., Chen, Z., Sun, H., Liao, H., Qin, S., Liu, W., Zhang, Y., Chen, Z., Zhou, S., 2022. Free radicals accelerate in situ ageing of microplastics during sludge composting. *J. Hazard. Mater.* 429,. <https://doi.org/10.1016/j.jhazmat.2022.128405> 128405.
- Yang, Y., Yang, J., Wu, W., Zhao, J., Song, Y., Gao, L., Yang, R., Jiang, L., 2015. Biodegradation and mineralization of polystyrene by plastic-eating mealworms: Part 2. Role of gut microorganisms. *Environ. Sci. Tech.* 49 (20), 12087–12093. <https://doi.org/10.1021/acs.est.5b02663>.
- Yang, Y., Chen, J., Chen, Z., Yu, Z., Xue, J., Luan, T., Chen, S., Zhou, S., 2022. Mechanisms of polystyrene microplastic degradation by the microbially driven Fenton reaction. *Water Res.* 223,. <https://doi.org/10.1016/j.watres.2022.118979> 118979.
- Zhang, X., Su, H., Gao, P., Li, B., Feng, L., Liu, Y., Du, Z., Zhang, L., 2022. Effects and mechanisms of aged polystyrene microplastics on the photodegradation of sulfamethoxazole in water under simulated sunlight. *J. Hazard. Mater.* 433,. <https://doi.org/10.1016/j.jhazmat.2022.128813> 128813.
- Zhu, K., Jia, H., Sun, Y., Dai, Y., Zhang, C., Guo, X., Wang, T., Zhu, L., 2020a. Long-term phototransformation of microplastics under simulated sunlight irradiation in aquatic environments: Roles of reactive oxygen species. *Water Res.* 173, 115564.
- Zhu, K., Jia, H., Sun, Y., Dai, Y., Zhang, C., Guo, X., Wang, T., Zhu, L., 2020b. Enhanced cytotoxicity of photoaged phenol-formaldehyde resins microplastics: combined effects of environmentally persistent free radicals, reactive oxygen species, and conjugated carbonyls. *Environ. Int.* 145, 106137.
- Zhu, K., Sun, Y., Jiang, W., Zhang, C., Dai, Y., Liu, Z., Wang, T., Guo, X., Jia, H., 2022. Inorganic anions influenced the photoaging kinetics and mechanism of polystyrene microplastic under the simulated sunlight: Role of reactive radical species. *Water Res.* 216,. <https://doi.org/10.1016/j.watres.2022.118294> 118294.